Research Article Open Access

Niko Guskos, Spiros Glenis, Grzegorz Zolnierkiewicz\*, Aleksander Guskos, Janusz Typek, Pawel Berczynski, Diana Dolat, Sylwia Mozia, and Antoni W. Morawski

# Magnetic properties of co-modified Fe,N-TiO<sub>2</sub> nanocomposites

**Abstract:** Iron and nitrogen co-modified titanium dioxide nanocomposites, nFe,N-TiO<sub>2</sub> (where n = 1, 5 and 10 wt% of Fe), were investigated by detailed dc susceptibility and magnetization measurements. Different kinds of magnetic interactions were evidenced depending essentially on iron loading of TiO<sub>2</sub>. The coexistence of superparamagnetic, paramagnetic and ferromagnetic phases was identified at high temperatures. Strong antiferromagnetic interactions were observed below 50 K, where some part of the nanocomposite entered into a long range antiferromagnetic ordering. Antiferromagnetic interactions were attributed to the magnetic agglomerates of iron-based and trivalent iron ions in FeTiO<sub>3</sub> phase, whereas ferromagnetic interactions stemmed from the F-center mediated bound magnetic polarons.

Keywords: titanium dioxide; magnetic property

PACS: 76.30.Fc, 81.07.Bc, 82.50.Hp

DOI 10.1515/phys-2015-0009 Received April 9, 2014; accepted July 28, 2014

1 Introduction

Recently, diluted magnetic semiconductors based on titanium dioxide ( $TiO_2$ ) doped with transition metal elements have been attracting particular attention due to the appearance of room temperature ferromagnetism [1–12],

of Physics, West Pomeranian University of Technology, Al. Piastow 48, 70-311 Szczecin, Poland, E-mail: gzolnierkiewicz@zut.edu.pl Spiros Glenis: Department of Solid State Physics, University of Athens, Panepistimioupolis, GR-157 84 Athens, Greece Niko Guskos, Aleksander Guskos, Janusz Typek, Pawel Berczynski: Department of Physics, West Pomeranian University of Technology, Al. Piastow 48, 70-311 Szczecin, Poland Diana Dolat, Sylwia Mozia, Antoni W. Morawski: Department of Chemical and Environmental Engineering, West Pomeranian University of Technology, Al. Piastow 17, 70-310 Szczecin, Poland

\*Corresponding Author: Grzegorz Zolnierkiewicz: Department

which may find applications in the field of spintronic and magneto-electronic devices. Furthermore, modification of titanium dioxide with a suitable choice of iron and nitrogen can significantly enhance the photocatalytic activity of titania under visible light [13]. Full understanding of the origin of room temperature ferromagnetism in TiO<sub>2</sub> materials is still lacking. Although bulk pure TiO<sub>2</sub> is diamagnetic, many studies have shown ferromagnetism of nanoscale TiO<sub>2</sub> due to the presence of oxygen vacancies on the surfaces and interfaces of studied samples [5]. Incorporation of transition metal elements (Fe<sup>3+</sup>, Cr<sup>3+</sup>, Ni<sup>3+</sup>, Co<sup>2+</sup>) in TiO<sub>2</sub> matrix at Ti<sup>4+</sup> sites should generate a considerable number of oxygen vacancies. The main question is whether the observed ferromagnetism is an extrinsic effect due to direct interaction between the local moments in magnetic impurity clusters or is it an intrinsic property caused by exchange coupling between the spin of the carriers and the local magnetic moments [7]. As the creation and distribution of the different concentrations of defects and formation of secondary ferromagnetic phases or metal clusters depends on the growth methods and the processing conditions of sample preparations it could also explain the inconsistent results obtained by different investigators. Electron paramagnetic resonance (EPR) and ferromagnetic resonance (FMR) have been frequently applied on doped and undoped TiO<sub>2</sub> to provide insight on the underlying spin dynamics and their physical properties responsible for possible applications [14–24]. FMR/EPR investigation of co-modified Fe,N-TiO<sub>2</sub> pointed to the coexistence of distinct magnetic centers and agglomerates that could be important for their photocatalytic activity [25].

The aim of this work was to study the static susceptibility and magnetization of three co-modified nFe,N-TiO $_2$  (n=1, 5, 10 wt% of Fe) nanopowders. As the magnetic interactions of agglomerates have an influence on the photocatalytic activity - especially in the visible region of electromagnetic radiation - the knowledge of magnetic properties of nFe,N-TiO $_2$  might help to unravel the mechanisms that establish the photocatalytic activity of titanium dioxide.

# 2 Experimental

Amorphous titanium dioxide (TiO2/A) from the sulfate technology supplied by Chemical Factory Police S.A. (Poland) was used as starting material for the synthesis of the (Fe,N) - co-modified rutile TiO<sub>2</sub> photocatalysts, as previously described [13]. A defined amount of TiO2 water suspension was stirred for 48 h in a beaker with appropriate amount of  $Fe(NO_3)_2$  so as the amount of Fe introduced to the beaker was of 1 wt%, 5 wt% or 10 wt% relatively to TiO2 content. Subsequently, samples were dried at 80°C for 24 h in an oven and annealed at 800°C in NH<sub>3</sub> flow (co-modified samples denoted as nFe,N-TiO<sub>2</sub>, where index n gives the wt% of Fe). The highest photocatalytic efficiency under visible light was measured for n=5 % nanocomposite, whereas the lowest photocatalytic performance was obtained for n=10 %. DC magnetization measurements were carried out using an MPMS-7 SQUID magnetometer in the 2-300 K temperature range and magnetic fields up to 70 kOe in the zero-field-cooling (ZFC) and field cooling (FC) modes.

## 3 Results and discussion

The XRD analysis confirmed complete transformation of anatase and amorphous phase to rutile as well as the presence of iron in the modified samples. In these samples iron is present mostly in the form of FeTiO $_3$  and in case of n=10 % sample - also as Fe $_3$ O $_4$  (see Fig.1). What is more, in n=1 % sample the presence of small amount of TiN phase was also revealed.

Figures 2 a-c present the temperature dependence of the dc magnetic susceptibility in the ZFC and FC modes for the nFe,N-TiO<sub>2</sub> (n=1, 5 and 10 %) samples measured at different magnetic fields. For all investigated nanocomposites, behavior of the magnetic susceptibility in ZFC and FC modes is very similar to what was observed for inhomogeneous magnetic agglomerate system comprising a low concentration of  $\gamma$ -Fe<sub>2</sub>O<sub>3</sub> agglomerates in non-magnetic matrices [26-28]. At low magnetic fields, the ZFC and FC modes deviate significantly in high temperatures range, while a broad, field dependent peak is observed at  $T_{max}$ in the ZFC susceptibility. In the case of non-interacting nanoparticles, this maximum marks the average blocking temperature of superparamagnetic moments at the time scale of the measurement, depending on the particle-size distribution [29, 30]. The dipolar and exchange interactions between nanoparticles could be responsible for the shift of  $T_{max}$  towards higher temperatures as well as the

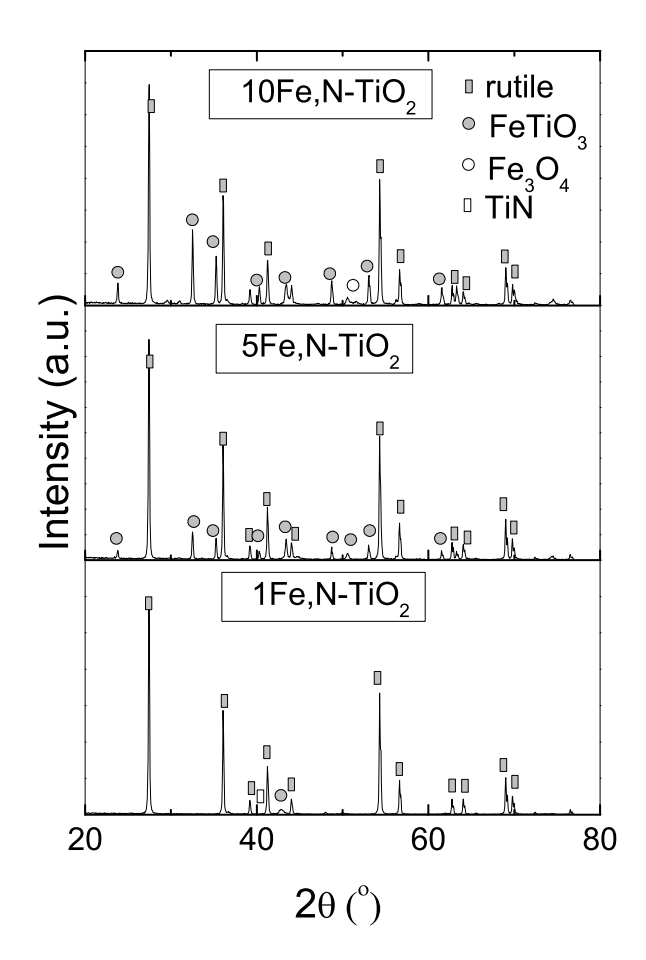


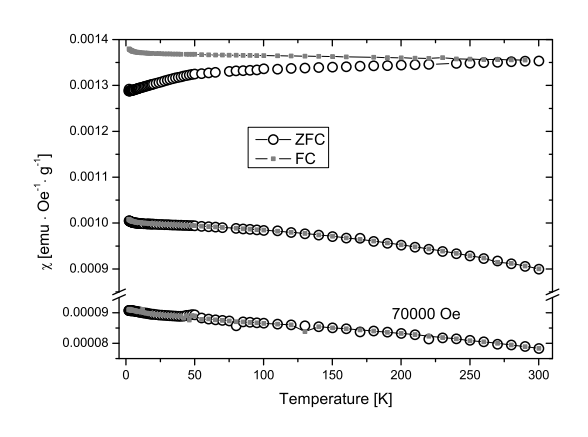
Figure 1: XRD patterns for three investigated  $nFe,N-TiO_2$  nanocomposites.

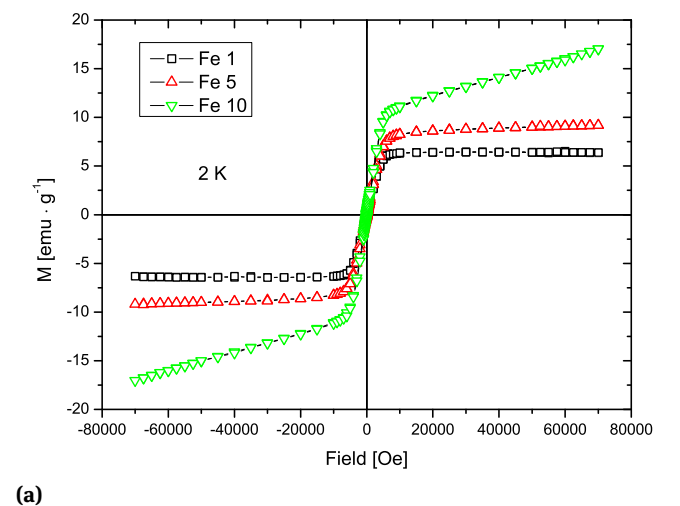
broadening of the  $M_{ZFC}$  peak and flattening of the ZFC/FC curves above  $T_{max}$ , pointing to a dominant magnetic interaction effect. At the highest magnetic field of 7 T, a peak of magnetic susceptibility emerged at 49, 48 and 54 K for the nanocomposites with n=1 %, 5 % and 10 %, respectively. This peak was most prominent for the n=10 % nanocomposite which was clearly observed even at low magnetic fields. The temperature dependence of the inverse FC magnetic susceptibility  $(1/\chi)$  for all investigated nanocomposites has shown a Curie-Weiss type behavior at high temperatures for all samples. The Curie-Weiss fit of  $\chi^{-1}(T)$  to the experimental data allowed to estimate the Curie-Weiss temperature  $(\theta)$  with negative values higher than 200 K, indicative of strong antiferromagnetic interactions.

Figures 3 a-b present the hysteresis loops for the three nanocomposites at 2 K and at room temperatures, and essential differences were recorded. The loops were fitted with one ferromagnetic and one paramagnetic component. The intersections on the field axis at increasing and

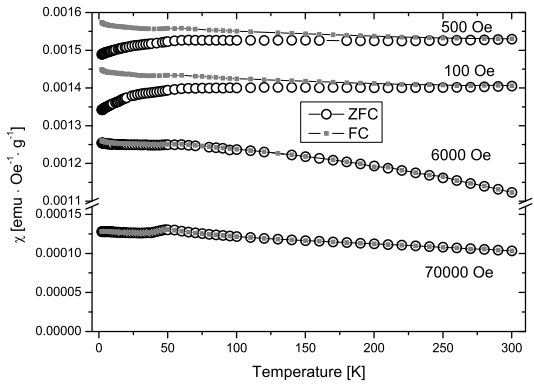
80 — N. Guskos *et al.* DE GRUYTER OPEN

(b)





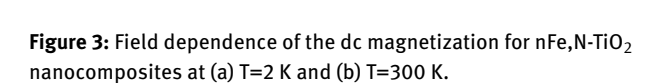
(a)

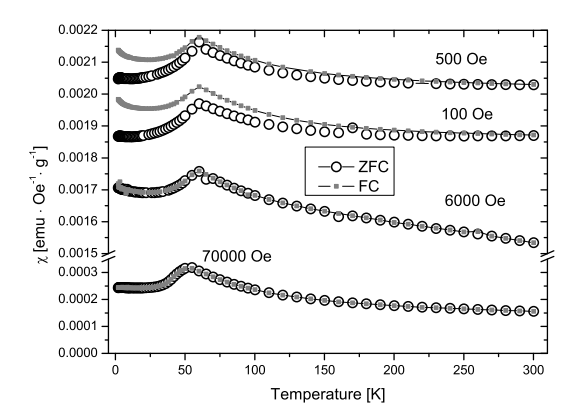


12 10 -□— Fe 1 -<u>△</u>— Fe 5 8 -⊽— Fe 10 6 -0-**0-**0-0-0-0-<del>0-0-0-0-</del> 4 300 K M [emu · g<sup>-1</sup>] 0 --2 -4 --6 -8 -10 -60000 -40000 -20000 20000 40000 60000 80000 Field [Oe]

(b)

(c)





decreasing fields ( $H_+$  are  $H_-$ ) in the FC hysteresis loop was used to estimate the coercive field ( $H_c$ ) as  $H_c$ =( $H_+$ - $H_-$ )/2.

**Figure 2:** Temperature dependence of the dc magnetic susceptibility for nFe,N-TiO $_2$  nanocomposites in ZFC and FC modes for different applied magnetic field: (a) n=1 %, (b) n=5 %, and (c) n=10 %.

Table 1 presents the saturation magnetization ( $M_s$ ), coercive field ( $H_c$ ) and remanence ( $M_r$ ) for the three nanocomposites nFe,N-TiO $_2$  at 2 K and 300 K. To make it more meaningful, the saturation magnetization and remanence are recalculated in Bohr magnetons per Fe ion. The saturation magnetization increased consistently with the iron loading and decreased with increasing temperature. For n=1 % sample the obtained value is equal to that for a spin only S=5/2 high-spin Fe $^{3+}$  ion ( $\sim$  6  $\mu$   $_B$ ). For samples with higher concentration of iron loading it is significantly smaller. At low temperatures, the coercive filed and remanence were higher for the nanocomposite with n=1 %, while at room temperature the differences were reduced. Moreover, sample n=5 % showed the lowest values of  $H_c$ 

0.012(5)

0.013(2)

Sample index n [wt%]	Temperature [K]	$M_s$		$M_r$		ц [0o]
		$\mu_B/\text{Fe}$	[emu/g]	$[\mu_B/\text{Fe}]$	[emu/g]	- H <sub>c</sub> [Oe]
1	2	6.1(2)	6.1(2)	0.20(2)	0.20(2)	136(2)
	300	5.7(2)	5.7(2)	0.11(2)	0.11(2)	70(2)
5	2	1.9(2)	9.3(3)	0.014(5)	0.07(1)	41(2)
	300	1.5(2)	7.3(3)	0.016(5)	0.08(1)	34(2)

1.1(2)

1.1(2)

10.9(3)

10.8(3)

2

300

**Table 1:** Saturation magnetization ( $M_s$ ), coercive field ( $H_c$ ) and remanence ( $M_r$ ) for three nanocomposites nFe,N-TiO<sub>2</sub> at two different temperatures.

and M<sub>r</sub> at both temperatures among the three nanocomposites. These results are very similar to what was observed in the case of Cr doped TiO<sub>2</sub> nanoparticles [5]. Thus our results could also be explained by invoking the same F-center mediated bound magnetic polarons (BMP) theory [31]. Substitution of Fe<sup>3+</sup> ion at Ti<sup>4+</sup> site produces oxygen vacancy and connected with it localized electron (F center). Electron spin of an F center interacts with that of the spins of the neighbouring Fe<sup>3+</sup> ion. Overlap of BMPs leads to the long range ferromagnetic order in the lattice of doped TiO<sub>2</sub> [5]. For small concentration of Fe<sup>3+</sup> ions, the increase of iron loading leads to increase in magnetization, but for larger iron concentrations not all Fe<sup>3+</sup> ions are associated with oxygen vacancies. Some could be involved in Fe<sup>3+</sup>-O<sup>2-</sup>-Fe<sup>3+</sup> bonds or even could form iron clusters. These interactions lead to antiparallel (antiferromagnetic) alignment of the spins and in result to effective reduction in magnetization for higher iron loadings.

10

According to the XRD analysis, all nFe,N-TiO2 nanocomposites crystallized in the rutile TiO<sub>2</sub> phase after calcination at 800°C under NH<sub>3</sub> flow [13], together with the formation of the FeTiO3 secondary phase as the iron loading increased in n=5% and 10% samples. Additionally, the presence of TiN and magnetite Fe<sub>3</sub>O<sub>4</sub> was identified for the composites with n=1 % and n=10 %, respectively. Introduction of iron in the sublattice of transition ions in TiO2 could result in appearance of ferromagnetic state as predicted by BMP theory [31]. FMR measurements have shown that Fe<sub>3</sub>O<sub>4</sub> could lead to the formation of small concentration of magnetic cluster acting like small nanoparticles [25, 32]. It is possible that magnetite was not identified by XRD for the nanocomposites with n=1 % and n=5 % because of the limited sensitivity of this method at low phase contents. Thus the magnetic properties of the nFe,N-TiO<sub>2</sub> nanocomposites could be accordingly attributed to the contribution of the external (the presence of FeTiO<sub>3</sub>, Fe<sub>3</sub>O<sub>4</sub> phases) and internal factors (BMP centers). In particular, Fe<sub>3</sub>O<sub>4</sub> forms a superparamagnetic state, whereas FeTiO<sub>3</sub> forms paramagnetic state. The hysteresis loop arises from the doped TiO<sub>2</sub> as the value of the remanence is very low. The main contribution to the bulk magnetization comes from iron ions in the ferromagnetic and paramagnetic phases. The iron ions of the FeTiO<sub>3</sub> phase are coupled to an antiferromagnetic long range ordered state below 50 K (Fig.2). Because the amount of the FeTiO<sub>3</sub> phase increases with the increase of iron loading, the presence of the corresponding peak is most evident for the n=10% nanocomposite. In that case, the saturation magnetization is almost the same at low and high temperatures (Table 1) because long range antiferromagnetic ordering in the FeTiO<sub>3</sub> essentially decreases its contribution to the magnetization at low temperatures. Magnetic measurements on ilmenite have recorded a Neel transition temperature, which ranged from 56 K to 57.7 K and the authors have suggested the coexistence of superparamagnetic and ferromagnetic states [33].

0.12(2)

0.13(2)

66(2)

63(2)

Concentration depended magnetic properties of Fedoped  $TiO_2$  have been recently investigated by ac magnetization and Mossbauer spectroscopy [9]. The results have shown the presence of ferromagnetic and paramagnetic interactions at room temperature. The saturation magnetization, unlike coercivity, of the ferromagnetic phase increased with the increase of the concentration of iron atoms, as in the present case. The decrease of the effective magnetic moment with iron loading was also observed and attributed to the precipitation of Fe rich antiferromagnetic structures.

### 4 Conclusions

The dc susceptibility and magnetization of three comodified nFe,N-TiO $_2$  (n=1, 5, 10 % of Fe) nanocomposites have been investigated and the results have shown the coexistence of different magnetic phases. A ferromagnetic phase was assigned to the iron doped titanium dioxide in form of F-center mediated bound magnetic polarons. The

bulk magnetization was dominated by the contribution of superparamagnetic and paramagnetic states with strong antiferromagnetic interactions arising from magnetic agglomerates and the FeTiO<sub>3</sub> ilmenite phase. The spins of ilmenite couple to a long range antiferromagnetic ordered state at about 50 K. The phase transition temperature and amounts of paramagnetic phases essentially depend on the concentration of iron ions.

**Acknowledgement:** This work was supported by National Centre for Science and Ministry of Science and Higher Education of Poland under decision No. 802/N-Japonia/2010/0. The authors would like to thank Professor Barbara Grzmil from West Pomeranian University of Technology, Szczecin for helpful assistance during XRD measurements.

### References

- [1] Z. Matsumoto et al., Science 291, 854 (2001)
- [2] Y. R. Park, S. Choi, J. H. Lee, and K. J. Kim, Kor. Phys. Soc. 50, 638 (2007)
- [3] H. Li, M. Liu, Y. Yeng, and T. Huang, J. Cent. South Univ. Tech. 17, 239 (2010)
- [4] Y. L. Zhao et al., Appl. Phys. Lett. 101, 142105 (2012)
- [5] B. Choudhury and A. Choudhury, Mat. Sci. Eng. B 178, 794 (2013)
- [6] G. Mallia, N. M. Harrison, Phys. Rev. B 75, 165201 (2007).
- [7] B. Santara, P. K. Giri, S. Dhara, K. Imakata, M. Fuji, J. Phys. D: Appl. Phys. 47, 235304 (2014)

- [8] D. Kim, J. Hong, Y. R. Park, K. J. Kim, J. Phys.: Condens. Matter 21, 195405 (2009)
- [9] A. M. Mudarra Navarro, V. Bilovol, A. F. Cabrera, C. E. Rodriguez Torres, Physica B 407, 3225 (2012)
- [10] M. Parras et al., J. Phys. Chem. Lett. 4. 2171 (2013)
- [11] I. Nakai et al., J. Korean Phys. Soc. 63, 532 (2013)
- [12] N. N. Bao, H. M. Fan, J. Ding, J. B. Yi, J. Appl. Phys. 109, 07C302 (2011)
- [13] D. Dolat, S. Mozia, B. Ohtani, and A. W. Morawski, Chem. Eng. J. 225, 358 (2013)
- [14] J. M. Coronado et al., Langmuir 17, 5368 (2001)
- [15] G. Mele et al., J. Phys. Chem. B 109, 12347 (2005)
- [16] S. Yang et al., Appl. Phys. Lett. 94, 162114 (2009)
- [17] B. Tiana et al., Chem. Eng. J., 151, 220 (2009)
- [18] F. D. Brandao, M. V. B. Pinheiro, G. M. Ribeiro, G. Medeiros-Ribeiro, and K. Krambrock, Phys. Rev B 80, 235204 (2009)
- [19] S. Yang, A. T. Brant, and L. E. Halliburton, Phys. Rev. B 82, 035209 (2010)
- [20] I. R. Macdonalda, R. F. Howea, X. Zhang, W. Zhou, J. Photochemistry and Photobiology. A: Chem., 216, 238 (2010)
- [21] I. A. Shkrob, T. W. Marin, S. D. Chemerisov, and M. D. Sewilla, J. Phys. Chem. C 115, 4642 (2011)
- [22] N. Guskos et al., Mater. Sci. Eng. B 177, 223 (2012)
- [23] N. Guskos et al., Mater. Chem. Phys. 136, 889 (2012)
- [24] N. Guskos et al., Central Eur. J. Chem. 11, 1994 (2003)
- [25] N. Guskos et al., J. Alloys Compd. 606, 32 (2014)
- [26] N. Guskos et al., J. Appl. Phys. 99, 084307 (2006)
- [27] N. Guskos et al., J. Non Cryst. Solids. 354, 4401 (2008)
- [28] N. Guskos et al., J. Nanosci. Nanotech. 8, 2127 (2008)
- [29] R. W. Chantrell, N. S. Walmsley, J. Gore, and M. Maylin, Phys. Rev. B 63, 024410 (2000)
- [30] P. P. Vaishnava et al., Phys. Rev. B 76, 024413 (2007)
- [31] M. J. Calderon, S. Das Sarma, Ann. Phys-New York 322, 2618 (2007)
- [32] N. Guskos et al., J. Appl. Phys. 97, 0204304 (2005)
- [33] F. E. Senftle et al., Earth Planet. Sci. Lett. 26, 377 (1975)